8.4 ANALYSIS OF TRACE-P OBSERVATIONS USING A FOUR-DIMENSIONAL VARIATIONAL DATA ASSIMILATION TECHNIQUE

Tianfeng Chai, *Gregory R. Carmichael
University of Iowa
Iowa City, Iowa

Dacian N. Daescu
Portland State University
Portland, Oregon

Adrian Sandu
Virginia Tech.
Blacksburg, Virginia

1 INTRODUCTION

Variational methods (3D-Var, 4D-Var) provide an optimal control approach to the data assimilation problem. Four-dimensional variational (4D-Var) data assimilation allows the optimal combination of three sources of information: an a priori ("background") estimate of the state of the atmosphere; knowledge about the physical and chemical processes that govern the evolution of pollutant fields, as captured in the model (CTM); and observations of some of the state variables. The optimal analysis state is obtained through a minimization process to provide the best fit to the background estimate and to all observational data (space and time distributed) available in the assimilation window. The use of the adjoint modeling to evaluate the gradient of the objective functional makes feasible the implementation of the 4D-Var data assimilation for large-scale atmospheric models.

The direct decoupled method has been extensively used for sensitivity studies in three dimensional (3D) atmospheric chemistry transport simulations (Yang *et al.*, 1998; Yang *et al.*, 2000; Hakamiand *et al.*, 2003). Direct sensitivity analysis via (forward mode) automatic differentiation was also employed in the context of photochemical transport models (Carmichael *et al.*, 1997; Huwang*et al.*, 1997; He *et al.*, 2000). Adjoint sensitivity is a complementary approach which efficiently calculates the derivatives of a functional with respect to a large number of parameters.

In this paper we present the mathematical theory of adjoint sensitivity analysis applied to three dimensional atmospheric transport and chemistry models. We discuss the computational tools developed and used to build the adjoint of a comprehensive 3D air quality model, including parallelization and performance of 3D adjoints. The use of adjoints for sensitivity analysis and for data assimilation problems is illustrated using numerical simulations of air pollution in East Asia during the TRACE-P (TRAnsport and Chemical Evolution over the Pacific) field campaign. The paper is organized as follows. In Section 2 we review the mathematical theory of adjoint sensitivity analysis applied to air quality modeling. Section 3 discusses implementation aspects. Numerical results for the simulation of East Asia are shown in Section 4. Conclusions and future research directions are given in Section 5.

2 MATHEMATICAL ASPECTS

In this section a review of the mathematical aspects of chemical transport modeling and adjoint sensitivity analysis is presented. Both the continuous and discrete adjoint approaches are described.

2.1 Chemical Transport Modeling

In what follows we denote by u the wind field vector, K the turbulent diffusivity tensor, ρ the air density in $moles/cm^3$, and c_i the mole-fraction concentration of chemical species i. The density of this species is $\rho\ c_i\ moles/cm^3$. Let $V_i^{\rm dep}$ be the deposition velocity of species i, Q_i the rate of surface emissions, and E_i the rate of elevated emissions for this species. The rate of chemical transformations f_i depends on absolute concentration values; the rate at which mole-fraction concentrations change is then $f_i(\rho c)/\rho$.

Consider a domain Ω which covers a region of the atmosphere. Let $\vec{n}$ be the outward normal vector on each point of the boundary $\partial\Omega$. At each time moment the boundary of the domain is partitioned into $\partial\Omega = \Gamma^{\rm IN} \cup \Gamma^{\rm OUT} \cup \Gamma^{\rm GR}$ where $\Gamma^{\rm GR}$ is the ground level portion of the boundary; $\Gamma^{\rm IN}$ is the set of (lateral or top) boundary points where $u\cdot\vec{n} \le 0$ and $\Gamma^{\rm OUT}$ the set where $u\cdot\vec{n} > 0$.

The evolution of c_i in time is described by the material balance equations

$$\frac{\partial c_i}{\partial t} = -u\cdot\nabla c_i + \frac{1}{\rho}\nabla\cdot\left(\rho K\nabla c_i\right) + \frac{1}{\rho} f_i(\rho c) + E_i\ , \quad t^0 \le t \le T, \tag{1}$$

$$c_i(t^0,x) = c_i^0(x)\ , \tag{2}$$

$$c_i(t,x) = c_i^{\rm IN}(t,x) \quad \text{for} \quad x\in\Gamma^{\rm IN}\ , \tag{3}$$

$$K\frac{\partial c_i}{\partial n} = 0 \quad \text{for} \quad x\in\Gamma^{\rm OUT}\ , \tag{4}$$

$$K\frac{\partial c_i}{\partial n} = V_i^{\rm dep} c_i - Q_i \quad \text{for} \quad x\in\Gamma^{\rm GR}\ . \tag{5}$$

We refer to the system (1)–(5) as the *forward (direct) model*. To simplify the presentation, in this paper we consider as parameters the initial state c^0 of the model; it is known that this does not restrict the generality of the formulation. The solution of the forward model $c = c(t,c^0)$ is uniquely determined once the model parameters c^0 are specified.

The direct model (1)–(5) is solved by a sequence of N timesteps of length Δt taken between t^0 and $t^N = T$. At each time step one calculates the numerical approximation $c^k(x) \approx c(t^k,x)$ at $t^k = t^0 + k\Delta t$ such that

$$c^{k+1} = \mathscr{N}_{[t^k,t^{k+1}]}\cdot c^k\ , \quad c^N = \prod_{k=0}^{N-1} \mathscr{N}_{[t^k,t^{k+1}]}\cdot c^0 \tag{6}$$

The numerical solution operator $\mathscr{N}$ is usually based on an operator splitting approach, where the transport steps along

*Corresponding author address: Tianfeng Chai, Center for Global and Regional Environmental Research, University of Iowa, Iowa City, IA 52242; e-mail: tchai@cgrer.uiowa.edu.

each direction and the chemistry steps are taken successively. Formally, if we denote by $\mathscr{T}$ the numerical solution operator for directional transport, and by $\mathscr{C}$ the solution operator for chemistry we have

$$\mathscr{N}_{[t,t+\Delta t]} = \mathscr{T}_X^{\Delta t/2} \cdot \mathscr{T}_Y^{\Delta t/2} \cdot \mathscr{T}_Z^{\Delta t/2} \cdot \mathscr{C}^{\Delta t} \cdot \mathscr{T}_Z^{\Delta t/2} \cdot \mathscr{T}_Y^{\Delta t/2} \cdot \mathscr{T}_X^{\Delta t/2} \tag{7}$$

2.2 Sensitivity Analysis

Consider a scalar cost functional defined using the model solution $c(t)$

$$\mathscr{J}(c^0) = \int_{t^0}^{T} dt \int_\Omega g\big(c(t,x)\big)\, dx \tag{8}$$

The cost functional depends implicitly on the parameters c^0 via the dependence of $c(t)$ on c^0. We want to compute the sensitivity of this functional with respect to the parameters,

$$\frac{\partial \mathscr{J}}{\partial c^0(x)} = \int_{t^0}^{T} dt \int_\Omega \frac{\partial g}{\partial c}\big(c(t,\xi)\big) \frac{\partial c(t,\xi)}{\partial c^0(x)} d\xi \tag{9}$$

This requires the sensitivities of the solution with respect to the parameters

$$S(t,x,\xi) = \frac{\partial c(t,\xi)}{\partial c^0(x)}\,, \qquad S(0,x,\xi) = \delta_{x-\xi} \tag{10}$$

2.2.1 Direct sensitivity analysis

An infinitesimal perturbation δc^0 in the parameters will result in perturbations $\delta c_i(t)$ of the concentration fields. These perturbations are solutions of the tangent linear model

$$\begin{aligned}
\frac{\partial \delta c_i}{\partial t} &= -u\cdot\nabla \delta c_i + \frac{1}{\rho}\nabla\cdot\big(\rho K \nabla \delta c_i\big) + F_{i,*}(\rho c)\,\delta c\,, \\
&\quad t^0 \le t \le T, && (11)\\
\delta c_i(t^0,x) &= \delta c_i^0(x)\,, && (12)\\
\delta c_i(t,x) &= \delta c_i^{\mathrm{IN}}(t,x) = 0 \quad \text{for} \quad x\in\Gamma^{\mathrm{IN}}\,, && (13)\\
K\frac{\partial \delta c_i}{\partial n} &= 0 \quad \text{for} \quad x\in\Gamma^{\mathrm{OUT}}\,, && (14)\\
K\frac{\partial \delta c_i}{\partial n} &= V_i^{\mathrm{dep}}\delta c_i \quad \text{for} \quad x\in\Gamma^{\mathrm{GR}}\,. && (15)
\end{aligned}$$

In the above F is the Jacobian of the function f, and $F_{i,*}$ denotes its i-th row. We refer to (11)–(15) as the *tangent linear model* associated with the forward model (1)–(5).

The sensitivities (10) link the solution perturbations with the initial perturbations via

$$\delta c(t,\xi) = S(t,x,\xi)\,\delta c^0(x) \tag{16}$$

In the direct sensitivity analysis approach one solves the model (1)–(5) together with the tangent linear model (11)–(15) forward in time. The equations (11)–(15) are of convection-diffusion-reaction type (with linearized chemistry) and in practice are solved by the same numerical method as the forward model (6)–(7); computational savings are possible by reusing the same matrix factorizations.

2.2.2 Continuous adjoint sensitivity analysis

The adjoint of the tangent linear model defines the evolution of the adjoint variables λ_i

$$\begin{aligned}
\frac{\partial \lambda_i}{\partial t} + \nabla\cdot(u\lambda_i) &= -\nabla\cdot\left(\rho K \nabla \frac{\lambda_i}{\rho}\right) - \Big(F^T(\rho c)\lambda\Big)_i \\
&\quad -\phi_i, \quad T \ge t \ge t^0, && (17)\\
\lambda_i(T,x) &= \lambda_i^F(x)\,, && (18)\\
\lambda_i(t,x) &= 0 \quad \text{for} \quad x\in\Gamma^{\mathrm{IN}}\,, && (19)\\
\lambda_i u + \rho K \frac{\partial(\lambda_i/\rho)}{\partial n} &= 0 \quad \text{for} \quad x\in\Gamma^{\mathrm{OUT}}\,, && (20)\\
\rho K \frac{\partial(\lambda_i/\rho)}{\partial n} &= V_i^{\mathrm{dep}}\lambda_i \quad \text{for} \quad x\in\Gamma^{\mathrm{GR}}\,. && (21)
\end{aligned}$$

To obtain the ground boundary condition we use the fact that $u\cdot n = 0$ at ground level. ϕ_i is a forcing function yet to be defined. We refer to (17)–(21) as the *(continuous) adjoint system* of the tangent linear model (11)–(15). Note that the adjoint initial condition is posed at the final time T.

The adjoint system (17)–(21) depends on the state of the forward model (i.e. on the concentration fields $c(x,t)$) through the nonlinear chemical term $F(\rho c)$ and possibly through the forcing term ϕ for nonlinear functionals. This means that the forward model must be first solved forward in time, the state $c(x,t)$ saved for all t, then the adjoint model could be integrated backwards in time from T down to t^0.

In practice a hybrid approach is used. The forward model is solved using a numerical method, and the numerical approximation of the state is saved periodically. These checkpoints are used in the definition of the adjoint equations. The continuous adjoint equation (17)–(21) is a convection-diffusion-reaction equation (with linearized chemistry) and can be solved by any numerical method of choice. In particular an operator splitting approach could be employed using the same numerical methods as for solving the direct model

$$\lambda^k = \mathscr{N}_{[t^{k+1},t^k]}\cdot\lambda^{k+1}\,, \quad \lambda^0 = \prod_{k=0}^{N-1} \mathscr{N}_{[t^{N-k},t^{N-k-1}]}\cdot\lambda^N \tag{22}$$

The forcing function ϕ_i and the initial values λ_i^F are chosen such that the adjoint variables are the sensitivities of the cost functional with respect to state variables (concentrations)

$$\lambda_i(x,t) = \frac{\partial \mathscr{J}}{\partial c_i(x,t)} \tag{23}$$

2.2.3 Discrete adjoint sensitivity analysis

In this approach the numerical discretization of the (1)–(5) is considered to be the forward model (6). This is a pragmatic view, as only the numerical model is in fact available for analysis. For brevity the state of the discretized model will be denoted $c_i^k[j]$, where i is the species index, j is the space discretization index and k the time discretization index. $c^k[j]$ will refer to the vector of all species at time level k and grid level j. The cost functional is defined in terms of the discrete model state

$$\mathscr{J}(c^0) = \sum_{k=0}^{N}\sum_j g\big(c^k[j]\big) \tag{24}$$

and one wants the derivatives of this functional with respect to the discrete model parameters $c_i^0[j]$. A perturbation δc^0 in the parameters c^0 propagates in time according to the tangent linear discrete equation

$$\delta c^{k+1} = \mathscr{N}'_{[t^k,t^{k+1}]} \cdot \delta c^k \,, \quad \delta c^N = \prod_{i=0}^{N-1} \mathscr{N}'_{[t^k,t^{k+1}]} \cdot \delta c^0 \quad (25)$$

where $\mathscr{N}'$ is the tangent linear operator associated with the solution operator $\mathscr{N}$. For an operator splitting approach (7) $\mathscr{N}'$ is built from the tangent linear transport and chemistry operators

$$\begin{aligned} \mathscr{N}'_{[t,t+\Delta t]} \quad = \quad & \mathscr{T}'^{\Delta t/2}_X \cdot \mathscr{T}'^{\Delta t/2}_Y \cdot \mathscr{T}'^{\Delta t/2}_Z \\ & \cdot \mathscr{C}'^{\Delta t} \cdot \mathscr{T}'^{\Delta t/2}_Z \cdot \mathscr{T}'^{\Delta t/2}_Y \cdot \mathscr{T}'^{\Delta t/2}_X \end{aligned} \quad (26)$$

To each tangent linear operator corresponds an adjoint operator (denoted here with a star superscript). The adjoint equation of (26) is

$$\begin{aligned} \mathscr{N}'^*_{[t+\Delta t,t]} \quad = \quad & \mathscr{T}'^{*\Delta t/2}_X \cdot \mathscr{T}'^{*\Delta t/2}_Y \cdot \mathscr{T}'^{*\Delta t/2}_Z \\ & \cdot \mathscr{C}'^{*\Delta t} \cdot \mathscr{T}'^{*\Delta t/2}_Z \cdot \mathscr{T}'^{*\Delta t/2}_Y \cdot \mathscr{T}'^{*\Delta t/2}_X \end{aligned} \quad (27)$$

such that the resulting *(discrete) adjoint model* is

$$\lambda^k = \mathscr{N}'^*_{[t^{k+1},t^k]} \cdot \lambda^{k+1} + \phi^{k+1} \,, \quad \lambda^N[j] = \lambda^F(x_j) \quad (28)$$

This approach was taken to build the adjoint of the 3D chemical transport model STEM. The exact formulation of discrete adjoint operators depends on the numerical methods employed to solve the forward model.

The forcing function ϕ and the initial values λ^N are chosen such that the adjoint variables are sensitivities of the functional with respect to the state variables

$$\lambda_i^k[j] = \frac{\partial \mathscr{J}(c^0)}{\partial c_i^k[j]} \quad (29)$$

3 IMPLEMENTATION

The forward and adjoint models are parallel and were run on a cluster of Linux workstations. Parallelization is based on dimensional splitting as supported by our library PAQMSG (Miehe *et al*. 2002) . The library supports data types for structured grids, and implements routines for data decomposition, allocation of local and global entities, data scattering, gathering, and shuffling. We use the horizontal-vertical data decomposition. With data in the horizontal slice format each processor can compute the horizontal transport; then data is shuffled in vertical column format and each processor can compute radiation, vertical transport, chemistry and aerosol processes in one column. The bulk of the computations is done with data in the column partitioned format; PAQMSG implements a static mapping scheme of columns (tasks) to processors that ensures an excellent load balancing. On a cluster of workstations all input and output is handled by the master process; and all computations are done by the worker nodes.

For the adjoint we use a two-level checkpointing scheme. The level-2 checkpoints store the concentration fields on the disk every 15 minutes, i.e. at every operator split step. Note that the linear transport scheme does not require any additional checkpointing storage. The amount of level-2 checkpoint data increases fivefold if a nonlinear transport scheme (e.g. using flux limiting) is used. The level-1 checkpoints store the concentrations for each process inside the 15 minutes intervals; level-1 checkpoints use memory buffers. For example one forward integration of each chemical box model for 15 minutes split time interval requires a number of smaller time steps; these intermediate concentrations are stored in a temporary matrix and used during the backward integration of the adjoint model. Operator splitting and the relative short split time intervals make it feasible to store the level-1 checkpoints in memory.

The gas phase chemical mechanism is SAPRC-99 (Carter, 2000) which considers the gas-phase atmospheric reactions of volatile organic (VOCs) and nitrogen oxides (NOx) in urban and regional settings. The forward time integration is done with the Rosenbrock numerical integrator Ros-2; the continuous adjoint model uses Ros-2 on the same sequence of steps as the forward chemical integration. Both the forward and the adjoint models are implemented using KPP.

For our East Asia application discussed in the following section the total level-2 checkpoint information stored is $\sim$ 162 MBytes of data for each hour of simulation; or $\sim$ 4 GBytes per 24 hours of simulation. The level-2 checkpoints of the parallel model are distributed in a manner where each node stores local information on the local disk. This takes full advantage of the total storage capabilities of the system. It also decreases the communication overhead when the parallel computation runs on a cluster of workstations since the gigabytes of data are not transmitted over the (relatively slow) connection. The distributed checkpointing strategy is therefore essential for both efficiency and overall storage capacity. Note that for the static domain decomposition implemented in PAQMSG the local entities (i.e. horizontal slices or sets of columns of the concentration field) have the same size throughout the computation, which makes the implementation of the distributed checkpointing scheme very efficient. For a dynamic domain decomposition strategy, on the other hand, the size of local entities change during the computation and the implementation of distributed checkpointing becomes complicated.

4 NUMERICAL RESULTS

The adjoint of the STEM chemical transport model can be used in sensitivity analysis studies and also for chemical data assimilation. We now present these two important applications of the computational tools developed. The analyzed problems are in support of large field experiments conducted in East Asia (i.e. TraceP). The simulated region is East Asia, and the simulated interval is one month starting at 0 GMT on March 1st, 2001. The meteorological fields are given by a dynamic meteorological model (RAMS), and the initial fields and boundary conditions correspond to Trace-P data campaign. The grid is $90 \times 60 \times 18$ points and has a horizontal resolution of $80\text{Km} \times 80\text{Km}$.

4.1 Adjoint Sensitivity Analysis

For the sensitivity analysis 10 simulation tests are carried out to cover the whole month of TraceP campaign period. They are listed in Table 1. The simulation interval for each case is three days. The first case starts at 0 : 00 GMT on March 1st, 2001, the second starts at 0 : 00 : 00 GMT on March 4th, 2001, and so forth. The response functional $g = g\big(c(t^F)\big)$ is the ground level ozone concentration at Cheju Island, at the final time step of each case.

As shown in Section 2, sensitivities of the response function $g = g\big(c(t^F)\big)$ with respect to the state variables (at each time instant) are the adjoint variables $\lambda(t)$, which can be obtained by integrating the adjoint model backwards in time. The distributions of the adjoint variables in the three-dimensional computation domain, which are available at any instant, provide the essential information for the sensitivity analysis. For instance, isosurfaces of adjoint variables delineate "influence regions", i.e. areas where perturbations in some concentrations will produce significant changes in the response functional (e.g. ozone at Cheju Island at the final time).

Results show that the influence regions are most affected by the meteorological fields. Figure 1 displays the influence areas of ozone (λ_{O_3}) at 24 hours before the final time in case 2 (March 4–6) and case 8 (March 22–26) respectively. The influence region for case 8 is toward the South and close to the Cheju Island, while that for case 2 is toward Northwest. This difference reflects different meteorological conditions, as indicated by the wind fields shown in Figure 1.

However, the influence regions are difficult to predict based solely on meteorological fields, due to the influence of turbulent diffusion and complicated chemical reactions. Because of the turbulent nature of the atmospheric boundary layer, the influence region may quickly extend to a very large area, covering most of the computational domain, and even beyond that. The fact that influence regions cannot be simply predicted through the meteorological fields is indicated by the differences in the influence regions of various chemical components, even if they are all driven by the same wind field. Figure 2 shows that influence regions of NO_2 and $HCHO$ at the same instant of case 1 (March 1–3) exhibit very different shapes, even if they are driven by the same wind field. This can be explained by the distinct roles of NO_2 and $HCHO$ in the ozone production.

4.2 Data Assimilation

Data assimilation means the integration of observational data and models with the goal of providing an optimal analysis state of the atmosphere. By optimal analysis state we mean an intimate and close integration of modeled and measured quantities, with the two merged together to provide the best estimate, physically consistent, of the evolving chemical state of the atmosphere. The analysis state better defines the spatial and temporal fields of key chemical components in relation to their sources and sinks.

The numerical results presented here correspond to the TraceP conditions starting at 0 : 00 GMT of March 1st, 2001. The data assimilation experiment is set using the twin experiments framework as follows:

- *Reference run*: The reference model run starts with the reference initial concentrations of all chemical species.
- *Observations and assimilation window*: We consider a 6 hours assimilation window. The observations are concentrations of selected species $Y_{\rm o}^{\rm obs}$ (here O_3 and NO_2) as computed by the reference run. Observations are provided on all grid points at the end of the assimilation window.
- *Parameters*: the control parameters are the initial concentrations of selected species $Y_{\rm c}(t^0)$ (here O_3 and NO_2).
- *Initial guess*: The reference initial values of the control species are increased by 20% to form the initial guess, which also serce as "background" values $Y_{\rm b}$.
- *Cost functional*: Measures the distance between the model predictions $Y_{\rm o}$ and the values $Y_{\rm o}^{\rm obs}$ of the selected observed species, as well as the deviation of control variables from the background state.

$$\begin{aligned} \mathscr{J}\big(Y_{\rm c}(t^0)\big) &= \frac{1}{2b}\sum[(Y_{\rm c}(t^0)-Y_{\rm b}]^2 \\ &+ \frac{1}{2r}\sum[Y_{\rm o}(t^F)-Y_{\rm o}^{\rm obs}(t^F)]^2 \end{aligned} \quad (30)$$

  where $b = 1000$ and $r = 1$. It means we trust the measurements considerably more than the background state.
- *Optimization algorithm*: Quasi-Newton limited memory L-BFGS (Byrd *et al.* 1995) . The optimization proceeds until the cost functional is reduced to 0.001 of its initial value, or the number of forward-backward model integrations exceeds 15.

We consider several scenarios, with the control variables being O_3 or NO_2, and the observed variables being O_3 and/or NO_2. The performance of the data assimilation procedure is measured by two indicators, the cost function value and the RMS error of control variables. The decrease in the cost function value versus the number of model runs during the optimization procedure is shown in Figure 3. The RMS errors

Table 1: Descriptions of the sensitivity analysis tests

Case	Simulation period	Target O_3 concenration
1	March 1-3, 2001	0 GMT on March 04, 2001
2	March 4-6, 2001	0 GMT on March 07, 2001
3	March 7-9, 2001	0 GMT on March 10, 2001
4	March 10-12, 2001	0 GMT on March 13, 2001
5	March 13-15, 2001	0 GMT on March 16, 2001
6	March 16-18, 2001	0 GMT on March 19, 2001
7	March 19-21, 2001	0 GMT on March 22, 2001
8	March 22-24, 2001	0 GMT on March 25, 2001
9	March 25-27, 2001	0 GMT on March 28, 2001
10	March 28-30, 2001	0 GMT on March 30, 2001

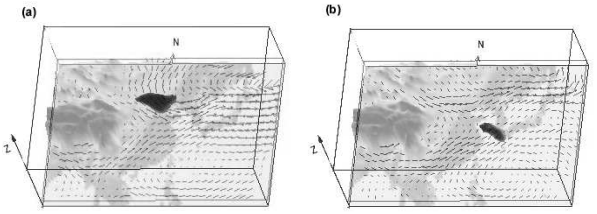

Figure 1: Influence areas of ozone on ozone at Cheju at 24 hours before the final time from (a) March 4–6, and (b) March 22–24. The isosurfaces of $\lambda_{O_3} = 0.001$ are shown as dark objects for both cases. Wind vectors at 2 *km* above the sea level are also shown over lightly gray-scaled topography. The differences in isosurface shapes and locations are due to differences in meteorological fields.

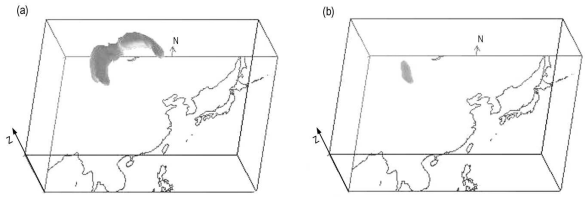

Figure 2: Influence ares of NO_2(a) and $HCHO$(b) for March 4–6, at 48 hours before the final time. The isosurfaces $\lambda_{NO_2} = 0.001$(a) and $\lambda_{HCHO} = 0.0001$(b) have different shapes due to the distinct roles NO_2 and $HCHO$ play in ozone production.

shown in Figure 4 measure the difference between the reference values of the control variables and their values recovered by data assimilation The decrease in the RMS error of control variables value versus the number of model runs during the optimization procedure is shown in Figure 4. With O_3 as control variables the optimization procedure produces a considerable decrease in the the cost function value, and a good decrease in the RMS error. Most of the information comes from O_3 observations; additional NO_2 observations do not seem to bring noticeable benefits. This may be due to the lack of scaling in our formulation of the cost functional. Ozone initial conditions seem to be recoverable through data assimilation. For comparison we include the optimization of the cost functional without the background term (corresponding to an infinite background covariance). As expected the cost function decreases further.

With NO_2 as control variables the decrease in the cost function, and in the RMS error, is not as pronounced. Again most of the information comes form O_3 measurements, with additional NO_2 measurements contributing very little to the optimization process. After about 10 model runs the RMS errors tend to stagnate, even if the cost functional continues to decrease. Perturbing the initial NO_2 concentration by 20% results in only a small change in the final (observed) O_3 concentration. This may be explained by the fact that NO_2 levels are driven mostly by emissions, and less by the initial conditions, which affects the observability of the initial NO_2 field through ozone measurements. The results indicate that further algorithmic developments are needed for assimilating NO_2. In particular a better scaling of the cost function, through a rigorous definition of the covariance matrices, is necessary.

5 CONCLUSIONS

In this paper we discuss the adjoint sensitivity analysis of three dimensional atmospheric transport and chemistry models. Adjoint modeling proves to be a powerful computational tool for sensitivity studies as well as for integrating observational data into the model in a four-dimensional variational (4D-Var) data assimilation procedure.

An overview of the mathematical theory of adjoint modeling applied to convection-diffusion-reaction models of atmospheric pollutants is given. The continuous and discrete adjoint model approaches are outlined, and formulations of the forcing terms for different cost functionals are discussed.

The use of adjoints for sensitivity analysis and for data assimilation problems is illustrated using numerical simulations of air pollution in East Asia. The analyzed problems are in support of the large TraceP experiment conducted in East Asia in March 2001.

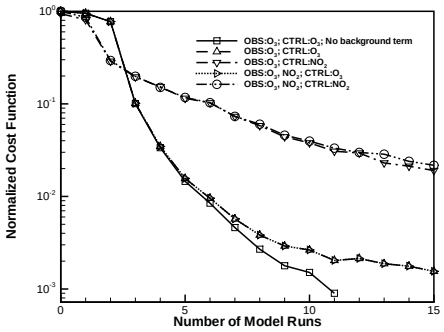

Figure 3: Data assimilation results: Cost function values (normalized by their pre-assimilation values) decrease during the optimization procedure. Several tests are shown using different control (CTRL) and observed (OBS) variables.

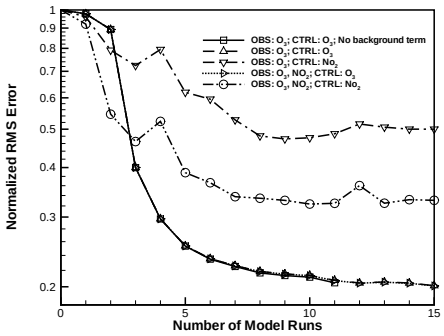

Figure 4: Data assimilation results: RMS errors of the control variables at the initial time (normalized by their pre-assimilation values) decrease during the optimization procedure. Several tests are shown using different control (CTRL) and observed (OBS) variables.

For sensitivity studies the target function is the ozone concentration at Cheju Island. Isosurfaces of adjoint variables delineate "influence regions", i.e. areas where perturbations in some concentrations will produce significant changes in this response functional. Results show that the influence regions are most affected by the meteorological fields, however they are difficult to predict from the meteorological information alone due to the influence of turbulent diffusion and complicated chemical reactions.

The data assimilation experiments are conducted in the twin experiment framework. We consider several scenarios, with the control variables being O_3 or NO_2, and the observed variables being O_3 and/or NO_2. The performance of the data assimilation procedure is measured by two indicators, the cost function value and the RMS error of control variables. The initial O_3 control variable can be recovered nicely from measurements through 4D-Var data assimilation. The recovery of the initial NO_2 concentrations is more difficult, presumably the fact that NO_2 levels are driven mostly by emissions.

Future work will focus on continuing the development of algorithmic and software infrastructure for adjoint modeling of comprehensive chemical transport models; and on using this computational infrastructure to run more complex tests and to assimilate real measurements data. The fundamental goal of this work is to enable the assimilation of chemical data available from ground, airplane, and satellite measurements into the models.

ACKNOWLEDGEMENTS

The authors thank the National Science Foundation for supporting this work through the award NSF ITR AP&IM 0205198.

References

Byrd, R., P. Lu, and J. Nocedal, 1995: A limited memory algorithm for bound constrained optimization. *SIAM J. Sci. Stat. Comput.*, **16**(5), 1190–1208.

Carmichael, G., A. Sandu, F. Potra, and V. Damian-Iordache, 1997: Sensitivity analysis for atmospheric chemistry models via automatic differentiation. *Atmospheric Environment*, **31**(3), 475–489.

Carter, W., 2000: Implementation of the saprc-99 chemical mechanism into the models-3 framework. Technical report, United States Environmental Protection Agency.

He, S., G. Carmichael, B. Hotchkiss, A. Sandu, and V. Damian-Iordache, 2000: Application of ADIFOR for air pollution model sensitivity studies. *Environment Modeling and software*, **15**, 549–557.

Hwang, D., D. Byun, and M. Odman, 1997: An automatic differentiation technique for sensitivity analysis of numerical advection schemes in air quality models. *Atmospheric Environment*, **31**(6), 879–888.

Miehe, P., A. Sandu, G. Carmichael, Y. Tang, and D. D. Odman, 2002: A communication library for the parallelization of air quality models. *Atmospheric Environment*, **36**(6), 3917–3930.

Odman, A. H. M. and A. Russell, 2003: High-order, direct sensitivity analysis of multidimensional air quality models. *Environmental Science and Technology*, **37**(11), 2442–2452.

Yang, Y., M. Odman, and A. Russell, 1998: Fast three-dimensional sensitivity analysis of photochemical air quality models: an application to southern California. *Proceedings of the Air and Waste Management Association's Annual Meeting and Exhibition*, **98-WP76A**(06), 2.

Yang, Y., J. Wilkinson, M. Odman, and A. Russell., 2000: Ozone sensitivity and uncertainty analysis using DDM-3D in a photochemical air quality model. *Air Pollution Modeling and its Application XIII: Proceedings of the 23rd NATO/CCMS International Technical Meeting on Air Pollution Modelling and Its Application*, **Varna, Bulgaria**, 183–194.